Contents
Previous Section

Porosity Prediction in Deeply Buried Sandstones, With Examples From Cretaceous Formations of the Rocky Mountain Region

By James W. Schmoker

GEOLOGIC CONTROLS OF DEEP NATURAL GAS RESOURCES IN THE UNITED STATES

U.S. GEOLOGICAL SURVEY BULLETIN 2146–H

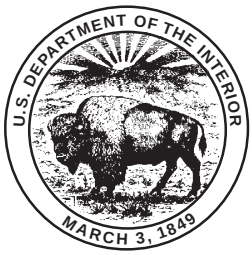

UNITED STATES GOVERNMENT PRINTING OFFICE, WASHINGTON : 1997

CONTENTS

FIGURES

TABLES

Porosity Prediction in Deeply Buried Sandstones, With Examples From Cretaceous Formations of the Rocky Mountain Region

By James W. Schmoker

ABSTRACT

Empirical porosity trends are examined for the Lower Cretaceous J sandstone in the Denver Basin, sandstones of the Upper Cretaceous Mesaverde Group in the Piceance and Uinta basins, and combined, undifferentiated Cretaceous sandstones in the Denver, Green River, Uinta, and Piceance basins. For each data set, porosity is examined as a function of vitrinite reflectance in an attempt to determine relations between porosity change during burial and thermal history. Correlations between porosity and internal hydrocarbon generation, carbonate cementation, clay content, and grain size are investigated as examples of links between porosity range at a given vitrinite reflectance level and causal geologic elements.

INTRODUCTION

Technology for drilling oil and gas wells below 15,000 ft (4,572 m) is well developed, and the ability to detect traps at these depths has improved steadily over the years. Nevertheless, in some deep basins of the United States, relatively few wells penetrate below 15,000 ft, and deeply buried sandstones in these basins are poorly explored.

One of the factors that has limited deep drilling for sandstone reservoirs is the knowledge that porosity can be too low to sustain economic hydrocarbon production. Better methods for estimating the porosity and porosity range of sandstones are needed for risk evaluation and reduction in deep-drilling programs, as well as for regional assessment of deep hydrocarbon resources.

In this report, I discuss an empirical approach to porosity prediction in deeply buried sandstones. Porosity trends are described as a function of thermal maturity, as represented by vitrinite reflectance (R_o). The porosity range at a given level of thermal maturity is predicted and is investigated as a function of rock properties such as clay content, carbonate cementation, and grain size and as a possible function of hydrocarbon generation.

Examples are drawn from Cretaceous sandstones of the Rocky Mountain region, including the Lower Cretaceous J sandstone (an informal unit of the Muddy Sandstone) of the Denver Basin, Colorado, and Upper Cretaceous sandstones of the Mesaverde Group of the Piceance and Uinta basins, Colorado and Utah. This paper is not intended as a report on the geology of these units. Rather, the J and Mesaverde sandstones serve to illustrate an approach to porosity prediction that has broad applicability to deeply buried sandstones. Cretaceous sandstones of Rocky Mountain basins are themselves not deeply buried in many of the areas studied but were chosen as analogs because of the availability of porosity, vitrinite reflectance, and petrographic data.

APPROACH TO POROSITY PREDICTION

Predictive sandstone porosity models should account for effects on porosity of rock properties and burial history. Simply relating porosity to rock properties, as is sometimes done in petrographic and core studies, may yield descriptive data that are difficult to generalize into regional predictive models.

The influence of burial history on porosity commonly has been represented by plots of porosity versus depth (Athy, 1930; Maxwell, 1964; Baldwin and Butler, 1985); however, in recent years, apparent relations between porosity and depth have come under critical review (van de Kamp, 1976; Lyons, 1978, 1979; Cassan and others, 1981; Siever, 1983; Scherer, 1987; Schmoker and Gautier, 1988, 1989; Keighin and others, 1989; Bloch, 1991). The point made in many of these latter papers is that processes of porosity modification during burial are strongly influenced by thermal history.

By plotting porosity as a function of vitrinite reflectance, which is a measure of thermal history, the effects of temporal and spatial variations in thermal gradient, subsidence, uplift, and erosion are normalized. Also, to the extent that vitrinite reflectance is time dependent, the duration of a given set of burial conditions is empirically taken into account.

Porosity-maturity relations, like porosity-depth curves, do not provide much insight into the processes causing porosity change in the subsurface. The influence on porosity of factors such as grain size and sorting, clay matrix, framework composition, early cementation, overpressuring, proximity to unconformities, dissolution (secondary porosity), and coating of framework grains is empirically taken into account by developing porosity–vitrinite reflectance trends that represent the 10th, 25th, 50th, 75th, and 90th porosity percentiles of data sets (fig. 1).

The 90th porosity percentile, for example, represents strata of the data set that have rock properties relatively favorable for pore-volume preservation or enhancement, whereas the 10th porosity percentile represents intervals of the data set that have properties favoring pore-volume reduction or occlusion at similar levels of thermal maturity. By depicting porosity using the 10th through 90th porosity percentiles (fig. 1), the porosity range at a given vitrinite reflectance level is taken into account. If porosity was reported only as an average, information significant for risk assessment, reservoir-engineering models, and volumetric calculations would be lost.

The dependence of sandstone porosity on vitrinite reflectance (R_o) can be represented by a power function of the form $\phi=A(R_o)^B$, where A and B (a negative number) are constants (Schmoker and Gautier, 1988, 1989). Such trends graph as straight-line segments on log-log plots.

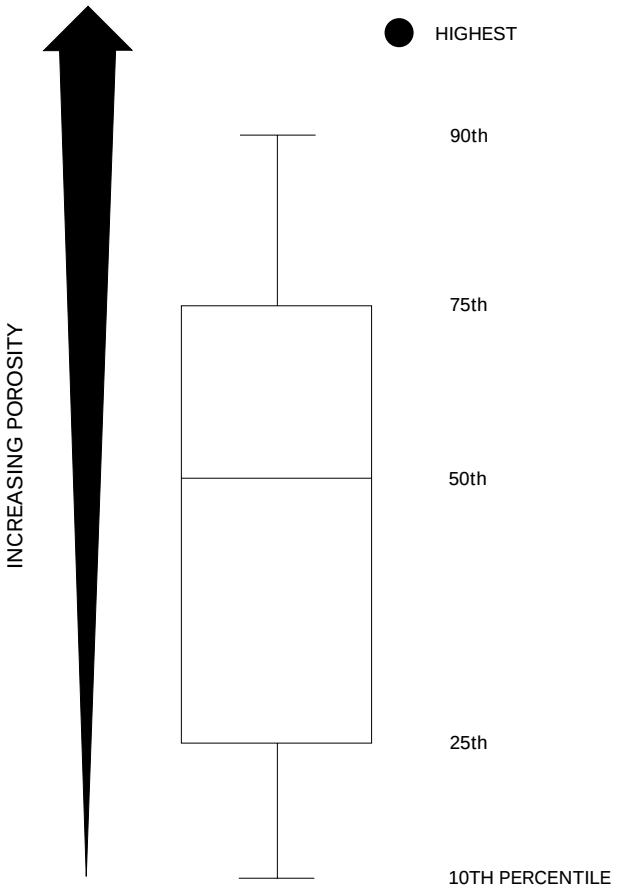

Figure 1. Box diagram illustrating data format used to develop porosity–vitrinite reflectance trends. Porosity distribution of each measurement suite is represented by 10th, 25th, 50th, 75th, and 90th porosity percentiles, as well as by single highest porosity measurement. Modified from Cleveland (1985).

PREDICTIVE POROSITY TRENDS FOR J SANDSTONE

The Lower Cretaceous J sandstone of the Dakota Group was deposited in nearshore-marine, deltaic, and fluvial-estuarine (valley-fill) settings in the Denver Basin (fig. 2). It is correlative to other Lower Cretaceous Dakota Group sandstones of the Rocky Mountain region (Coalson, 1989). Some 90 percent of the oil and gas extracted from the Denver Basin has been produced from the J sandstone (Land and Weimer, 1978; Tainter, 1984).

The maximum depth of the J sandstone in the wells of this study (fig. 2) is only 8,745 ft (2,665 m), at first consideration not sufficiently deep for the development of deep-sandstone porosity models; however, a good suite of porosity, vitrinite reflectance, and thin section data (Schmoker and Higley, 1991) makes the J sandstone a useful unit for developing approaches to porosity prediction. Such approaches might then be applied to sandstones in general. This section focusing on the J sandstone is based on work of Schmoker and Higley (1991), in which complete tables of the data used herein are presented.

POROSITY-MATURITY TRENDS

Core-plug porosity data from 31 wells in the Denver Basin (fig. 2) were used to create the porosity-vitrinite reflectance plots of figures 3 and 4. Vitrinite reflectance values were measured in each well by M.J. Pawlewicz, U.S. Geological Survey, using material from shale within and adjacent to the J sandstone. Because formation thickness does not exceed 150 ft (46 m) and is generally less than 100 ft (30 m), the thermal maturity of the J sandstone in an individual well does not vary significantly.

For the J sandstone, as well as for the other examples presented herein, the porosity data of a given measurement suite (such as data from a particular well) are grouped into a

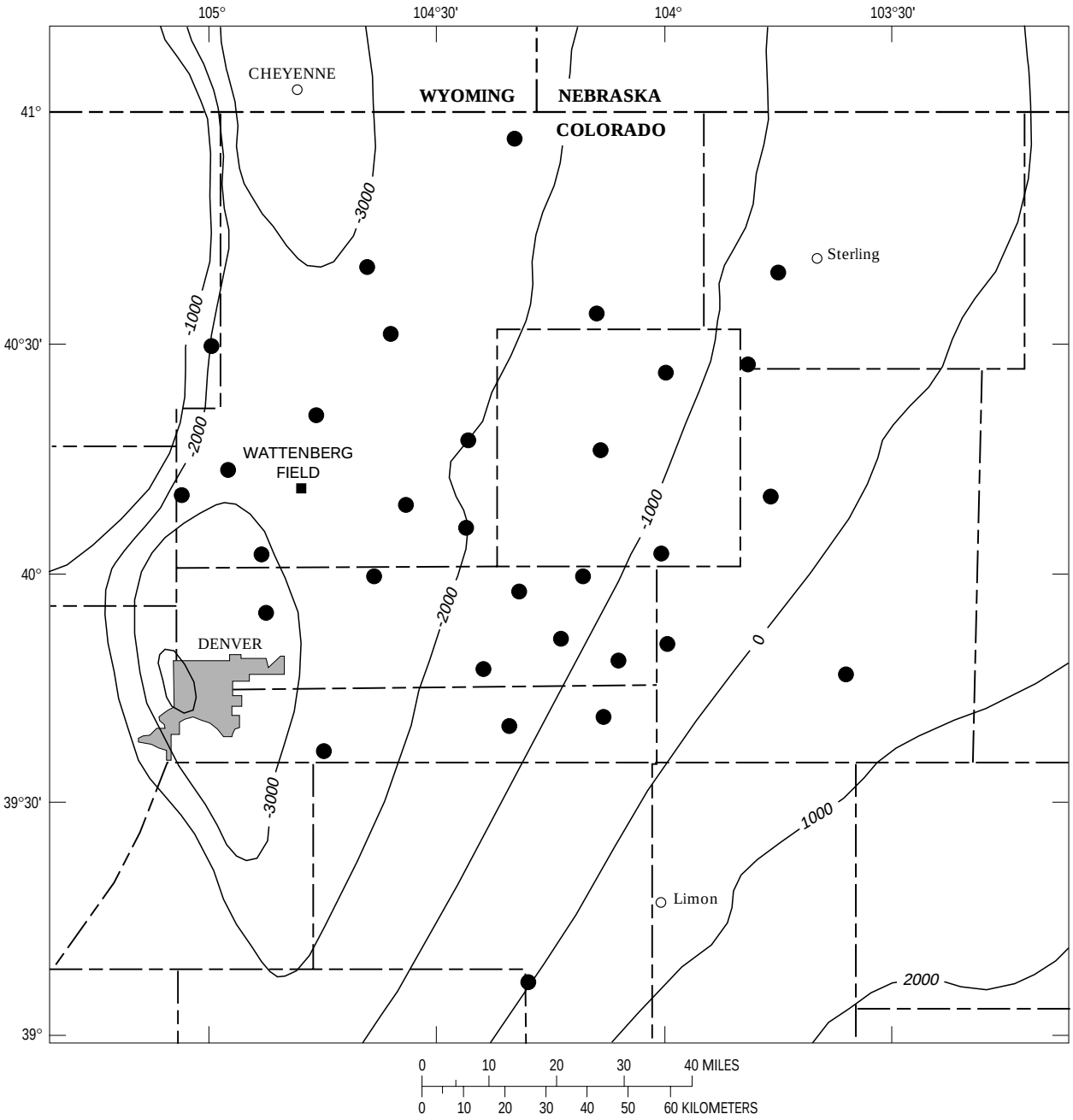

Figure 2. Map of study area in Denver Basin, Colorado, showing location of wells (solid circles) from which J sandstone porosity and vitrinite reflectance data were obtained. Structure contours are on top of J sandstone using sea-level datum (after Higley and Schmoker, 1989); contour interval 1,000 ft (305 m).

box diagram and represented by the 10th, 25th, 50th, 75th, and 90th porosity percentiles, as previously discussed (fig. 1). The porosity of the J sandstone is characterized by 31 such box diagrams.

Figure 3 shows the 50th (median) percentiles of the 31 J sandstone box diagrams, plotted as a function of vitrinite reflectance. A least-squares power-law regression line with vitrinite reflectance as the independent variable is fit to the data of this figure. Similar plots were made for the 10th, 25th, 75th, and 90th porosity percentiles. The porosity–vitrinite reflectance regression lines of these five plots are assembled in figure 4 and documented in table 1. Correlation coefficients range between –0.76 and –0.88. For 31 data points, a correlation coefficient of –0.42 would be significant at the 1 percent level (Till, 1974).

A power-function relation of porosity to vitrinite reflectance explains about three-fourths of the porosity variance of the 50th, 75th, and 90th J sandstone porosity percentiles

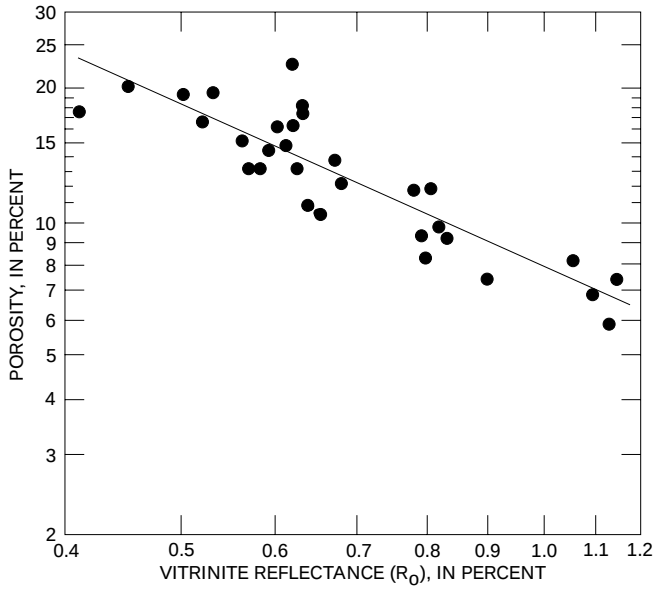

Figure 3. Porosity versus vitrinite reflectance for 50th percentile of J sandstone porosity distributions for 31 wells in Denver Basin. Coefficients for least-squares fit to data (line) are given in table 1. Location of wells is shown in figure 2.

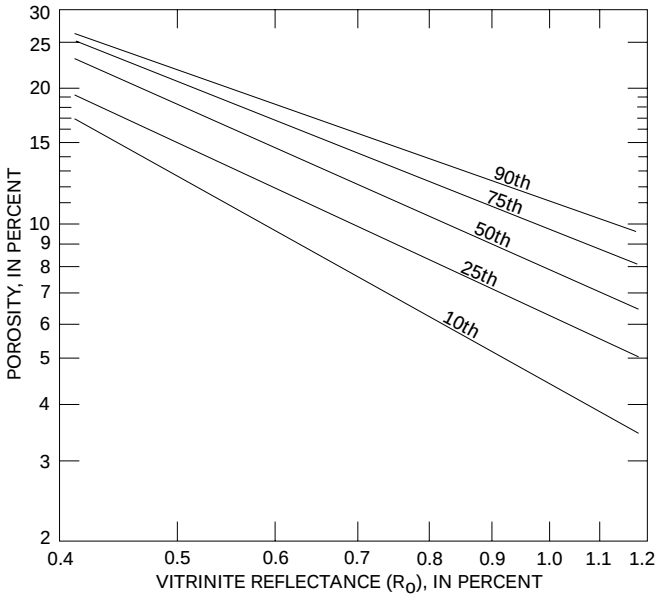

Figure 4. Porosity versus vitrinite reflectance regression lines for 10th, 25th, 50th, 75th, and 90th porosity percentiles, J sandstone, Denver Basin. Regression lines are documented in table 1. These trend lines constitute an empirical, predictive porosity model for the J sandstone.

(table 1). For these sandstones, the effect of thermal maturity on porosity change in the subsurface is considerably larger than that of all other factors combined.

The five regression lines of figure 4 each show a decrease of porosity with increasing thermal maturity.

Table 1. Power-law regression lines fit to J sandstone porosity–vitrinite reflectance data.
[Data are shown graphically in figure 4. 68 percent confidence intervals are shown for A and B]

Porosity percentile	$\phi=A(R_o)^B$ A	B	Correlation coefficient (r)	Fraction of total variance (r^2)
10th	4.6±0.5	–1.46±0.23	–0.76	0.58
25th	6.4±0.5	–1.23±0.17	–0.81	0.66
50th	8.1±0.5	–1.18±0.12	–0.88	0.77
75th	9.9±0.5	–1.05±0.12	–0.86	0.75
90th	11.4±0.6	–0.94 ±0.12	–0.83	0.69

Although the 10th through 90th porosity-percentile trends represent different combinations of diagenetic processes and geologic factors, the negative correlation between porosity and thermal maturity is characteristic of each case.

The trend lines of figure 4 provide an empirical framework for estimating both the porosity and the porosity range of the J sandstone within the Denver Basin. It is important to note, however, that the concept behind figure 4 is broader than a study of a particular sandstone in a particular basin. Figure 4 illustrates a sound general approach to empirical porosity prediction in sandstones.

POROSITY RANGE AT A GIVEN VITRINITE REFLECTANCE LEVEL

The predictive porosity model of figure 4 incorporates the porosity range at a given level of thermal maturity. Although a substantial porosity range at a given vitrinite reflectance level is typical of sandstones in general, the particular causal factors are varied and cannot be specified independently of observation. Examination of thin sections reveals that the petrographic factors that most affect J sandstone porosity variability at a given vitrinite reflectance level are carbonate cementation and clay content. These two factors are discussed briefly in the following paragraphs, as examples of the links between empirical porosity percentiles and causal geologic elements.

Carbonate cement, where present, reduces porosity. In addition, corroded and embayed quartz edges show that carbonate cement was formerly more widespread. Such cement protects the pore network from volume loss due to other processes of burial diagenesis relative to uncemented intervals. Thus, direct and indirect effects of carbonate cementation are responsible for a portion of the porosity range at a given vitrinite reflectance level shown in figure 4.

Abundant clay reduces J sandstone porosity, all else being equal, by occupying pores and deforming during

burial to fill pore networks. Low clay content also reduces porosity of the J sandstone, all else being equal, probably because inhibiting effects of clay on quartz cementation are mostly absent. Thus, the higher J sandstone porosities at a given R_o tend to be associated with intervals of intermediate clay content, that is, a clay content sufficient to retard quartz cementation yet low enough to minimize the mechanical clogging of pores (fig. 5). The clay content associated with maximum porosity percentile is about 12 percent in the J sandstone (fig. 5).

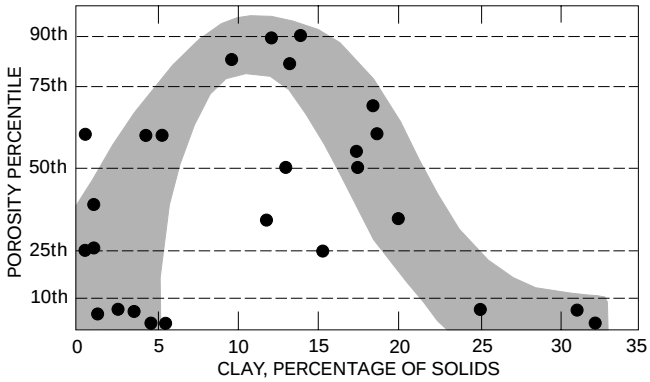

Figure 5. Point-count porosity, expressed relative to porosity-percentile trend lines of figure 4, versus clay content, J sandstone, Denver Basin. Interpretation of basic trend is shaded. For purposes of this figure, clay is defined as mudstone clasts, detrital clay, and authigenic mixed-layer illite-smectite and chlorite.

An important aspect of figure 5, one that extends beyond the characterization of the J sandstone, is that the vertical axis represents porosity percentile, rather than porosity, on an absolute scale. Thus, porosity is adjusted for the level of thermal maturity. This technique permits the crossplotting of porosity and petrographic measurements from rocks of different thermal maturity levels. The influence of geologic elements on porosity evolution in the subsurface can thus be isolated from the influence of burial history as represented by thermal maturity.

PREDICTIVE POROSITY TRENDS FOR MESAVERDE GROUP SANDSTONES

Upper Cretaceous, undifferentiated, predominantly nonmarine sandstones of the Mesaverde Group in the Piceance and Uinta basins contain large volumes of natural gas; however, economically successful exploration in these low-permeability fractured rocks has proven difficult. In large parts of the two basins, the Cretaceous section is

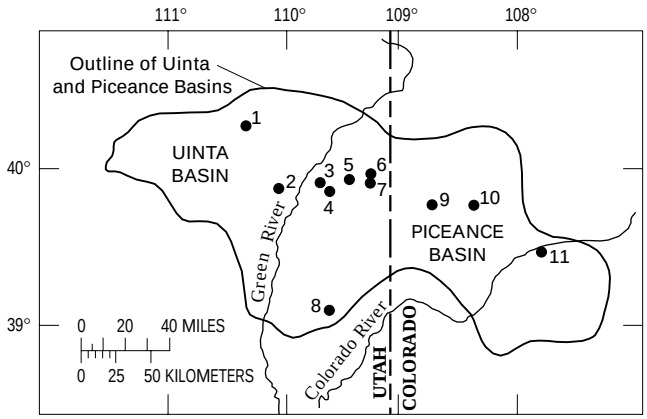

Figure 6. Map of Piceance and Uinta basins, Colorado and Utah, showing location of wells (solid circles) from which porosity data representing sandstones of Mesaverde Group were obtained.

sparsely drilled, and patterns of deposition, fracturing, and reservoir quality are not well known.

The maximum depth of Mesaverde sandstones in the wells of this study (fig. 6) in the Piceance Basin is 7,300 ft (2,230 m), whereas in one well in the Uinta Basin the Mesaverde is deeper than 15,000 ft (4,572 m). As with the preceding J sandstone example, the exercise of developing predictive porosity models for Mesaverde sandstones is intended to illustrate approaches that can be applied to sandstones in general. This section focusing on Mesaverde sandstones is based on work of Schmoker and others (1992), in which the data used here are discussed more fully.

POROSITY-MATURITY TRENDS

Core-plug porosity data from 14 wells (11 locations) in the Piceance and Uinta basins (fig. 6) are used for the porosity–vitrinite reflectance plots of figures 7 and 8. Vitrinite reflectance values were estimated in each well, based on core-plug depths, by interpolating from a variety of published and unpublished sources (Schmoker and others, 1992). The merging of data from the Piceance and Uinta basins is rationalized on the basis that Mesaverde rocks of both basins are temporally and depositionally similar (Keighin and Fouch, 1981). As in the case of the J sandstone, the porosity distribution of a given measurement suite is represented by porosity percentiles (fig. 1). The porosity of predominantly nonmarine Mesaverde sandstones is characterized by 31 box diagrams.

Figure 7 shows the 25th and 75th percentiles (connected by vertical lines) of the 31 Mesaverde box diagrams, plotted as a function of vitrinite reflectance. These data depict the middle range of porosity measurements and thus define an envelope of typical, or normal, porosities. Porosity-vitrinite reflectance trend lines

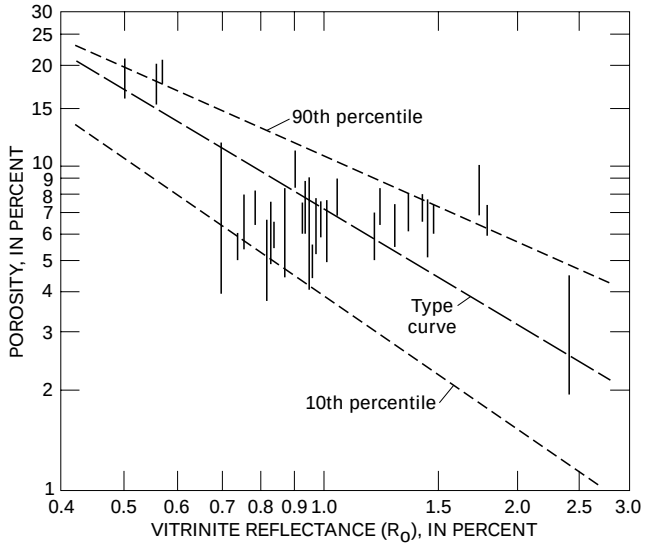

Figure 7. Porosity versus vitrinite reflectance for 25th through 75th percentiles (vertical lines) of porosity distributions for 31 samples of sandstone of the Mesaverde Group from 11 locations in Piceance and Uinta basins. Type curve, 10th percentile, and 90th percentile dashed lines provide a reference framework that represents sandstones in general (Schmoker and Gautier, 1989; Schmoker and Hester, 1990). Sample locations are shown in figure 6.

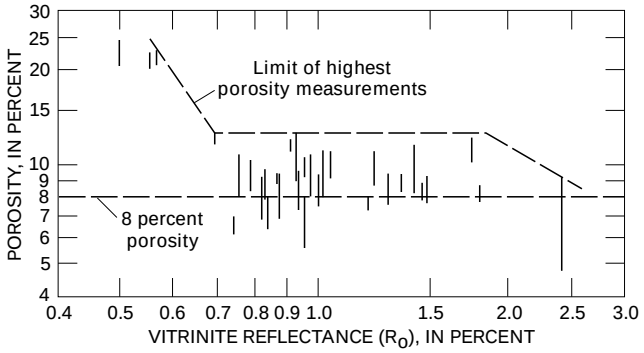

Figure 8. Porosity versus vitrinite reflectance for 75th percentiles through single highest measurements (vertical lines) of porosity distributions for 31 samples of sandstone of the Mesaverde Group from 11 locations in the Piceance and Uinta basins. Sample locations are shown in figure 6.

representing combined data sets of other formations are also shown in figure 7. The dashed line labeled "type curve" was presented by Schmoker and Gautier (1989) as a typical porosity versus thermal maturity curve for clastic rocks. The dashed lines labeled "10th percentile" and "90th percentile" are from Schmoker and Hester (1990) and form an envelope that encompasses 80 percent of their porosity data from various basins and formations. These three trend lines provide a reference framework against which to compare Mesaverde porosities.

Porosities of predominantly nonmarine Mesaverde sandstones have been described as low relative to other sandstones; however, comparison to the reference lines of figure 7 demonstrates that this is not the general case if levels of time-temperature exposure (vitrinite reflectance) are taken into consideration. In sharp contrast to J sandstone porosities, which decrease systematically as vitrinite reflectance increases (figs. 3, 4), the middle porosity range of Mesaverde sandstones does not show an overall porosity decrease between R_o of 0.7 and 1.8 percent (fig. 7). Whether casual or causal, these vitrinite reflectance levels approximate the window of active hydrocarbon generation (Tissot and Welte, 1984) for the type III kerogen present in nonmarine parts of the Mesaverde Group. Between R_o of 0.7 and 1.8 percent, Mesaverde sandstones have typical porosities in the 5–8 percent range (fig. 7).

Figure 8 shows the 75th percentiles and the single highest measurements (connected by vertical lines) of the 31 Mesaverde box diagrams, plotted as a function of vitrinite reflectance. These data depict the upper quartile of porosity measurements and thus define an envelope of above average porosities. Two reference lines (dashed) are also shown in figure 8. One marks the 8 percent porosity level, which is sometimes taken as an arbitrary lower cutoff for sandstone reservoirs, and the other approximates the high-porosity limit of the data set.

The distribution of upper quartile Mesaverde porosities (fig. 8) is similar in overall shape to that of the middle range of Mesaverde porosities (fig. 7). For vitrinite reflectance between 0.7 and 1.8 percent, Mesaverde sandstones are likely to have some intervals in which porosity is greater than 8 percent; the maximum porosity in this thermal maturity range is about 13 percent (fig. 8).

Models for the porosity and porosity range of the J and Mesaverde sandstones predict quite different responses of porosity to increasing thermal maturity (figs. 4, 7, 8); however, both models result from the same empirical method of porosity prediction. This method is robust and offers a sound general approach to the problem of porosity prediction in deeply buried sandstones.

POROSITY RANGE AT A GIVEN VITRINITE REFLECTANCE LEVEL

The predictive porosity model of figures 7 and 8 incorporates the porosity range at a given level of thermal maturity. Petrographic data indicate that proximity to the unconformity at the top of the Mesaverde Group, dissolution of early carbonate cement, larger grain size, and lower clay-matrix content are all factors favoring higher porosities in Mesaverde sandstones. These factors are discussed as additional examples of the links between empirical porosity percentiles and causal geologic elements.

Secondary porosity is probably best developed immediately below the Tertiary-Cretaceous unconformity at the top of the Mesaverde Group, and enhanced dissolution may be associated with surface weathering (Hansley and Johnson, 1990). The unconformity might also have enhanced later stage dissolution, in the subsurface, by focusing the flow of basin waters.

Porosities of Mesaverde sandstones greater than a few percent are unlikely if carbonate cement (determined by point-counting thin sections) exceeds about 12 percent. As in the case of the J sandstone, carbonate cement might have been widespread in intervals that now have little such cement. Early carbonate cement could preserve the pore network from mechanical and chemical compaction during burial relative to uncemented intervals; carbonate-cement dissolution could then develop relatively high, secondary porosity.

Grain size can influence the rate and extent of burial diagenesis (Houseknecht, 1984, and references therein). Data to test for a relation between grain size and porosity in Mesaverde sandstones are plotted in figure 9. The porosity ranges of the different grain-size categories are large and overlap; however, the midpoint porosity of each porosity range increases as grain size increases. These data (fig. 9) indicate a weak relation between grain size and porosity and suggest porosity that is higher in sandstones of larger grain size.

Data to test for a relation between clay-matrix content and porosity in Mesaverde sandstones are plotted in figure 10. Pseudomatrix and authigenic clays resulting from matrix recrystallization are included, to some extent, in the category of clay-matrix content. In contrast to the J sandstone (fig. 5), figure 10 shows no evidence of an association between optimum porosity and intermediate clay content. Although a predictive relation between clay-matrix content and porosity cannot be proposed for the Mesaverde, maximum porosity decreases systematically as matrix content increases (fig. 10). Porosities greater than a few percent are improbable if clay-matrix content exceeds 8 percent.

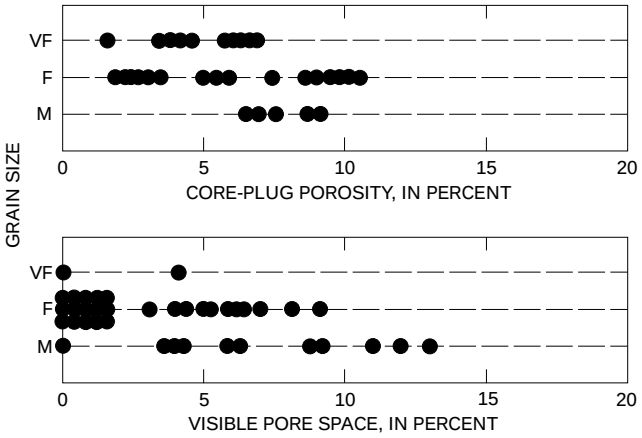

Figure 9. Core-plug porosity and visible pore space (as determined from point counting) as a function of grain size for Mesaverde Group sandstones from Colorado Interstate Gas Exploration Natural Buttes 21 well, sec. 15, T. 10 S., R. 22 E., Uintah County, Utah (loc. 5, fig. 6) (Pitman and others, 1986, 1987). Grain size: VF, very fine, 62–125 microns (micrometers); F, fine, 125–250 microns; M, medium, 250–500 microns.

The examples of the J and Mesaverde sandstones show how effects of geologic factors on porosity range can be incorporated within a thermal maturity framework.

PREDICTIVE POROSITY TRENDS FOR UNDIFFERENTIATED CRETACEOUS SANDSTONES OF ROCKY MOUNTAIN REGION

Porosity and vitrinite reflectance data from Cretaceous sandstones of Rocky Mountain basins can be combined to develop generic, regional models for porosity as a function of vitrinite reflectance. As in the examples of preceding sections, which focus on individual formations, the development of a predictive porosity model for Cretaceous sandstones of the Rocky Mountain region is intended primarily to illustrate approaches that can be applied to sandstones in general and to deeply buried sandstones in particular.

The Cretaceous data set described in table 2 represents formations in five different basins, a variety of geologic settings, and a wide range of thermal maturities and depths. The J sandstone and Mesaverde Group measurement suites of the preceding sections make up 58 percent of the combined Cretaceous data set.

Ideally, the measurement suites assembled here would represent a comprehensive sampling of all Rocky Mountain Cretaceous sandstones; however, in reality the data set is limited (table 2). Furthermore, wells in these basins are drilled according to specific selection criteria and do not provide an unbiased sampling of the subsurface. Nevertheless, the data set is thought to be sufficient to illustrate characteristics of generic, regional models for porosity and porosity range in which porosity predictivity is based on the level of thermal exposure.

POROSITY–THERMAL MATURITY TRENDS

Vitrinite reflectance is proportional to thermal exposure, which strongly influences burial diagenesis (Siever, 1983), and, as a result, porosity data from basins of varied temperature distributions and burial histories can be combined using vitrinite reflectance as the independent variable of comparison. Depth is sometimes used as the comparison variable, on the implicit assumption that depth is a direct measure of thermal history. Although this assumption is

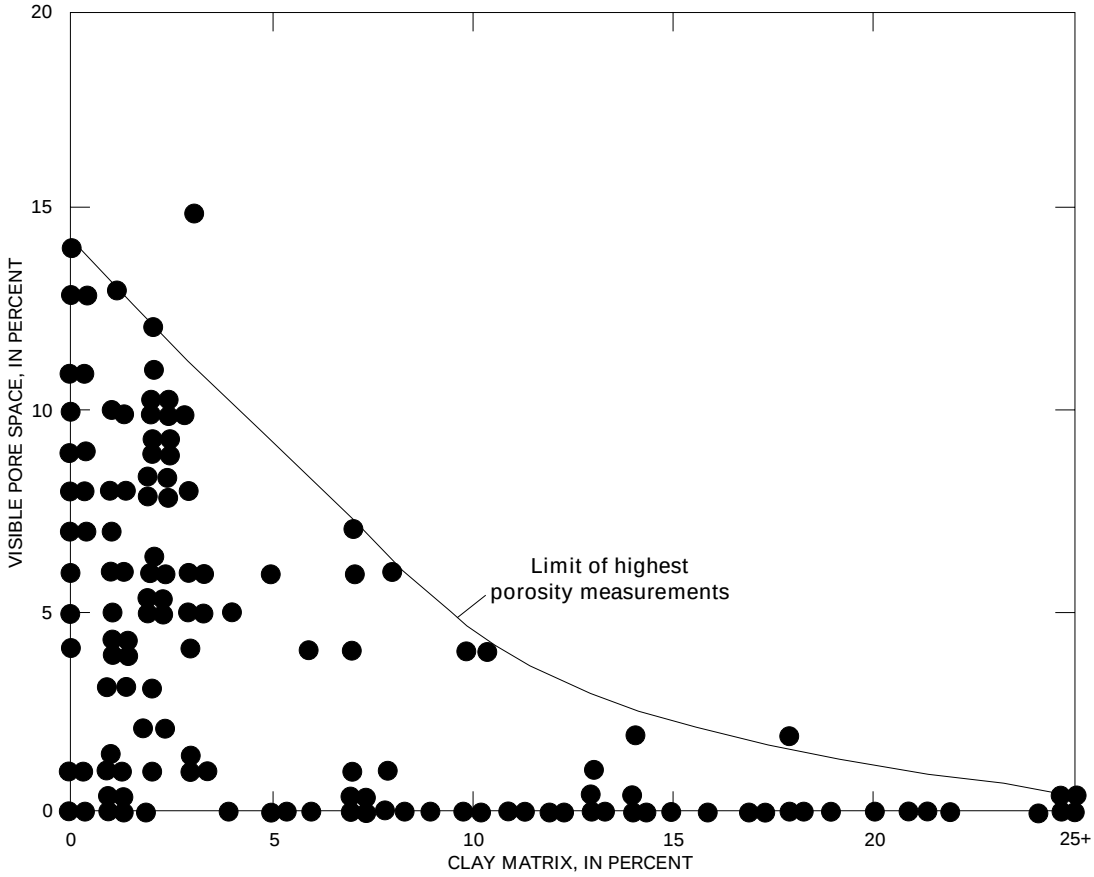

Figure 10. Point-count data showing visible pore space as a function of clay-matrix content for Mesaverde Group sandstones, from Colorado Interstate Gas Exploration Natural Buttes 21 well (sec. 15, T. 10 S., R. 22 E., Uintah County, Utah) (loc. 5, fig. 6) and Exxon Wilkin Ridge 1 well (sec. 29, T. 10 S., R. 17 E., Duchesne County, Utah) (loc. 2, fig. 6) (Pitman and others, 1988). Because vitrinite reflectance values for Mesaverde rocks in these two wells are similar (0.75–0.95 percent), porosity need not be expressed relative to porosity-percentile trend lines as in figure 5.

valid for some geologic settings, it is invalid for Rocky Mountain basins. As shown in figure 11, vitrinite reflectance cannot be accurately predicted on the basis of present-day depth within and between Rocky Mountain basins.

Present depth is not a good measure of thermal history in these basins and is therefore not a good parameter for combining the diverse Cretaceous sandstone porosity data of this study.

The 10th, 25th, 50th, 75th, and 90th percentiles (fig. 1) of 107 box diagrams, representing Cretaceous sandstones in the Denver, Green River, Powder River, Uinta, and Piceance Basins (table 2), are plotted as a function of vitrinite reflectance in figures 12–16. For each porosity percentile, an overall decrease of porosity with increasing vitrinite reflectance is apparent. Least-squares power-law regression lines with vitrinite reflectance as the independent variable are fit to the data of figures 12–16 (table 3). Correlation coefficients range between –0.60 and –0.76 (table 3). These correlation coefficients are somewhat lower than those for the J sandstone data set (table 1), as might be expected because of the greater geologic diversity and range of thermal maturity of the regional Cretaceous data set. For 107 data points, a correlation coefficient of –0.22 would be significant at the 1 percent level (Till, 1974).

The fraction of the total variance explained by the regression lines of figures 12–16 increases from 0.36 for the 10th porosity percentile to 0.58 for the 90th percentile. The higher porosity percentiles are thus modeled with more confidence than the lower percentiles. A power-function relation of porosity to vitrinite reflectance explains slightly more than half of the porosity variance of the 50th, 75th, and 90th percentiles (table 3). For these diverse Rocky Mountain Cretaceous sandstones, the effect of thermal exposure on porosity change in the subsurface is at least equal to that of all other factors combined.

The porosity-vitrinite reflectance regression lines of figures 12–16 together provide a possible empirical framework for estimating the porosity and the porosity range of

Table 2. Description of Cretaceous sandstone data set, Rocky Mountain basins.

Basin	Description and source	No. of core-plug porosity measurements	No. of measurement suites	Vitrinite reflectance (percent)	Depth (feet and meters)
Denver	J sandstone (Schmoker and Higley, 1991)	963	31*	0.41–1.14	4,300–8,700 (1,311–2,652)
Green River	Dakota Sandstone of Bridger Lake field (B.E. Law, written commun., 1987)	326	1	0.59	15,500 (4,724)
	Undifferentiated Cretaceous strata of El Paso Wagon Wheel 1 well (author's data)	442	7	0.66–1.78	8,100–16,100 (2,469–4,907)
	Almond Formation (B.E. Law, written commun., 1988)	811	24	0.57–1.64	4,500–14,300 (1,372–4,359)
Powder River	Sussex Sandstone Member of Cody Shale (D.K. Higley, written commun., 1991)	632	3	0.52–0.76	7,200–10,000 (2,195–3,048)
Uinta	Predominantly nonmarine sandstones of Mesaverde Group (Schmoker and others, 1992)	318	13*	0.56–2.40	700–19,300 (213–5,883)
Piceance	Predominantly nonmarine sandstones of Mesaverde Group (Schmoker and others, 1992)	741	18*	0.54–1.80	1,100–7,300 (335–2,225)
	Predominantly marine sandstones of Mesaverde Group (author's data; Schmoker and others, 1992)	162	6	1.33–2.16	7,500–8,200 (2,286–2,499)
	"B" zone of Mancos Shale (author's data)	67	4	1.80	11,800 (3,597)
	Total	4,462	107		

*Data used in discussions of porosity trends (this paper) for J or Mesaverde Group sandstones.

Cretaceous sandstones in Rocky Mountain basins (fig. 17). The Cretaceous sandstone porosity model of figure 17 is analogous in concept and similar in overall appearance to the J sandstone porosity model (fig. 4); however, the two porosity models differ in detail.

First, the five regression-line slopes of figure 17 are equal, within error limits, whereas those of the J sandstone porosity model decrease systematically as porosity percentile increases. Second, the 50th-percentile regression-line slope of figure 17 is less steep than that of the J sandstone porosity model and is also less steep than the "type curve" that is typical of other sandstone data sets.

Examination of the relation between the regression lines of figures 12–16 and the data points from which they are derived reveals the principal reason for the differences between the J sandstone (fig. 4) and the possible Rocky Mountain Cretaceous sandstone (fig. 17) porosity models. For vitrinite reflectance less than about 0.7 percent and greater than about 1.2 percent, the regression lines systematically underestimate actual porosity values, whereas between R_o of about 0.7 and 1.2 percent the regression lines systematically overestimate the actual porosity values (figs. 12–16). Thus, variations about the regression lines are not random. Although the correlation coefficients are fairly high, single regression lines fit to the entire vitrinite reflectance range do not reflect the internal structure of the Rocky Mountain Cretaceous sandstone data set.

ALTERNATIVE POROSITY MODEL

A second possible empirical approach for estimating the porosity and the porosity range of Cretaceous sandstones

Table 3. Power-law regression lines fit to combined Rocky Mountain porosity-vitrinite reflectance data.
[Data are shown graphically in figures 12–16. 68 percent confidence intervals are shown for A and B]

Porosity percentile	$\phi=A(R_o)^B$ A	B	Correlation coefficient (r)	Fraction of total variance ($r2$)
10th	5.0±0.3	–0.92±0.12	–0.60	0.36
25th	6.5±0.3	–0.90± 0.10	–0.66	0.44
50th	7.9±0.3	–0.93± 0.09	–0.72	0.52
75th	9.3±0.3	–0.88±0.08	–0.74	0.55
90th	10.5±0.3	–0.85±0.07	–0.76	0.58

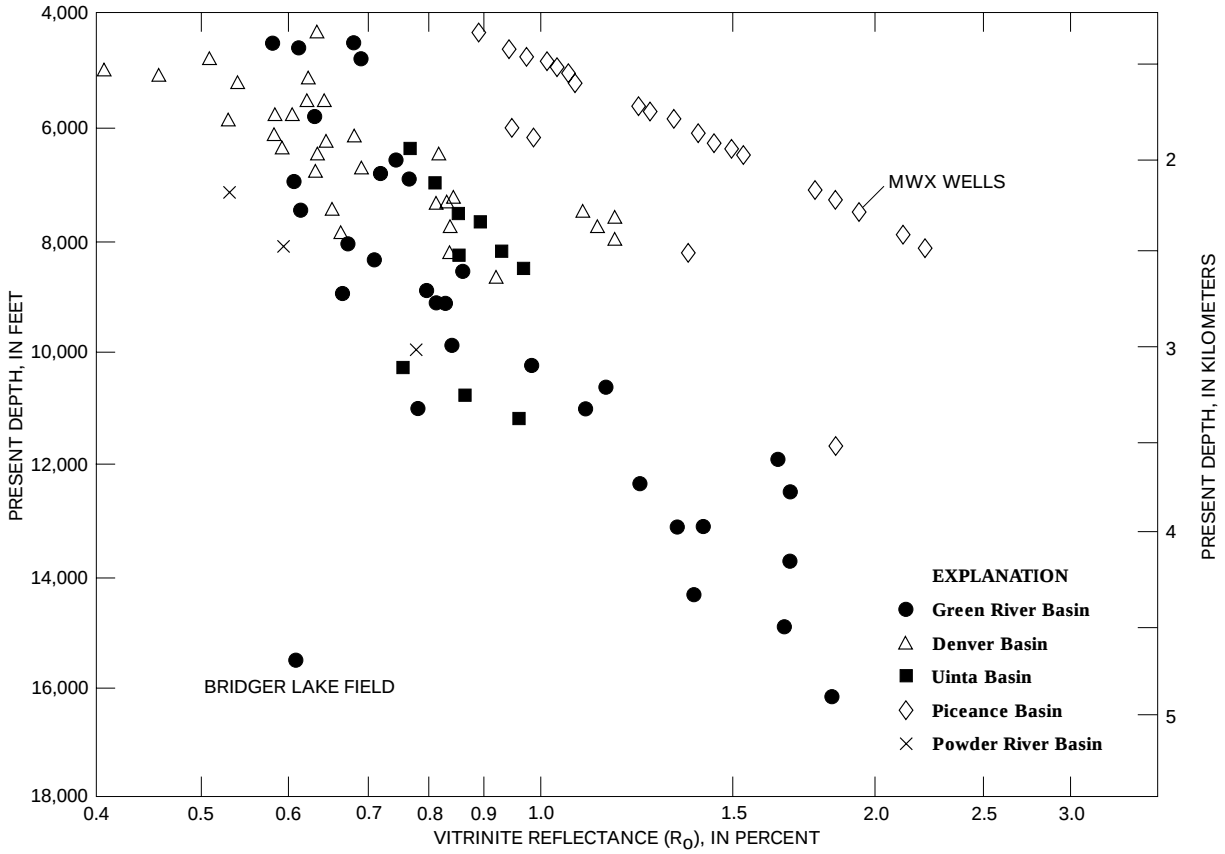

Figure 11. Present-day depth versus vitrinite reflectance for rocks of Cretaceous sandstone data set, Rocky Mountain basins (table 2). Trend labeled "MWX wells" refers to U.S. Department of Energy Multiwell Experiment, Garfield County, Colorado (Spencer and Keighin, 1984). Present depth of rocks at a given reflectance value can vary by many thousands of feet because of intra- and interbasinal variations in thermal and burial histories.

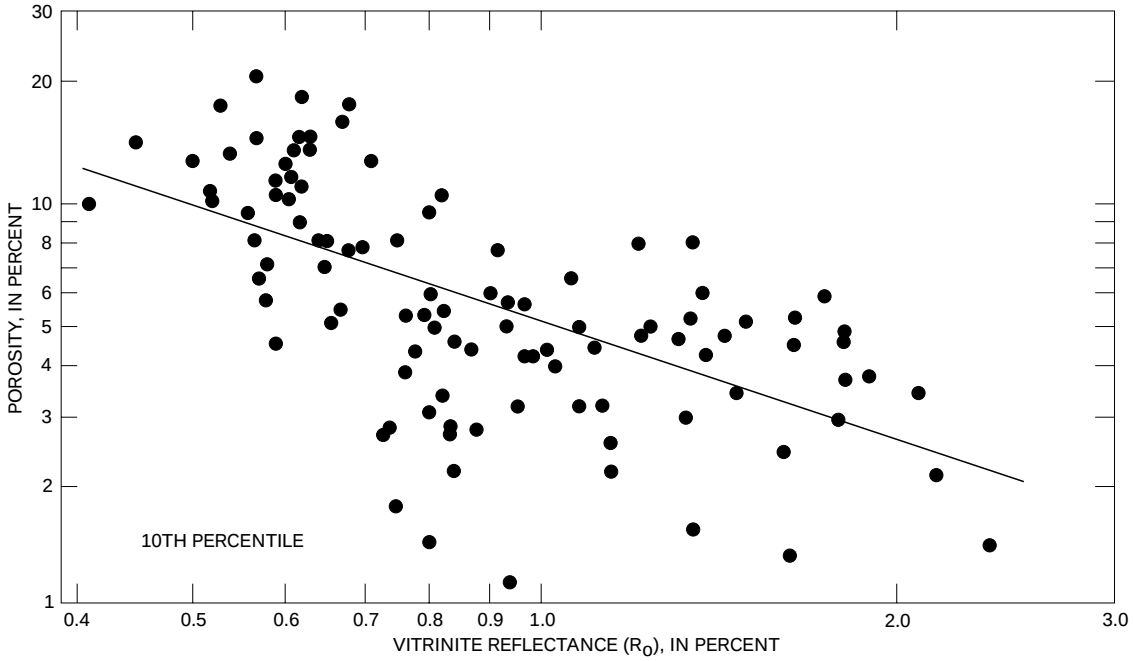

Figure 12. Porosity versus vitrinite reflectance for 10th percentile of Cretaceous sandstone data set, Rocky Mountain basins (table 2). Parameters for least-squares fit to data (line) are given in table 3.

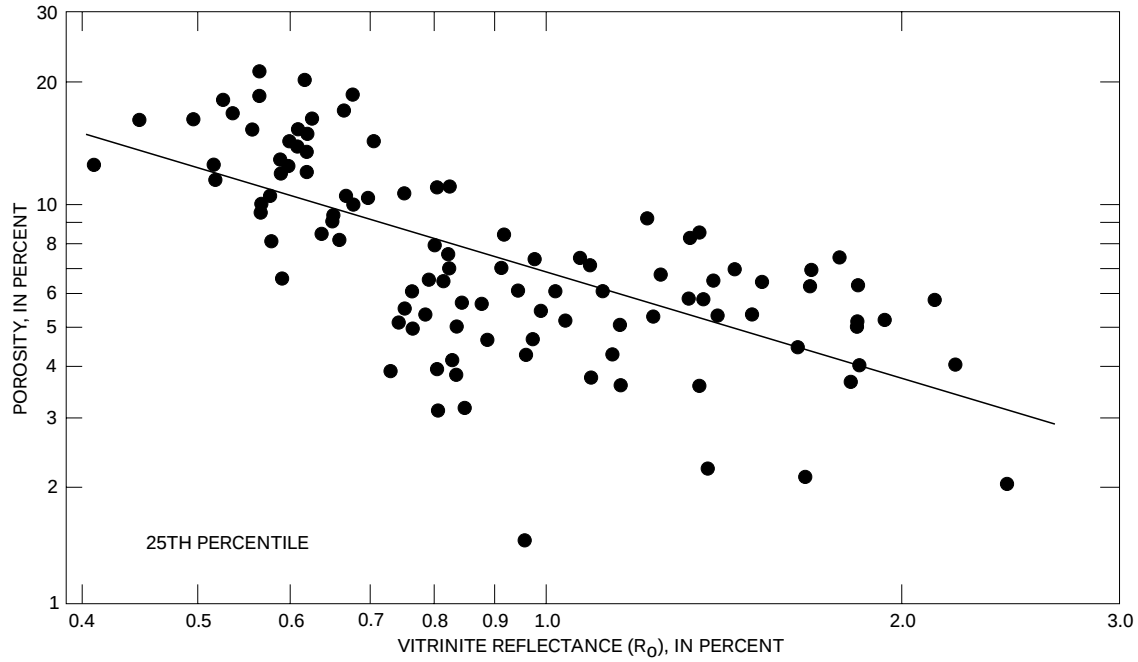

Figure 13. Porosity versus vitrinite reflectance for 25th percentile of Cretaceous sandstone data set, Rocky Mountain basins (table 2). Parameters for least-squares fit to data (line) are given in table 3.

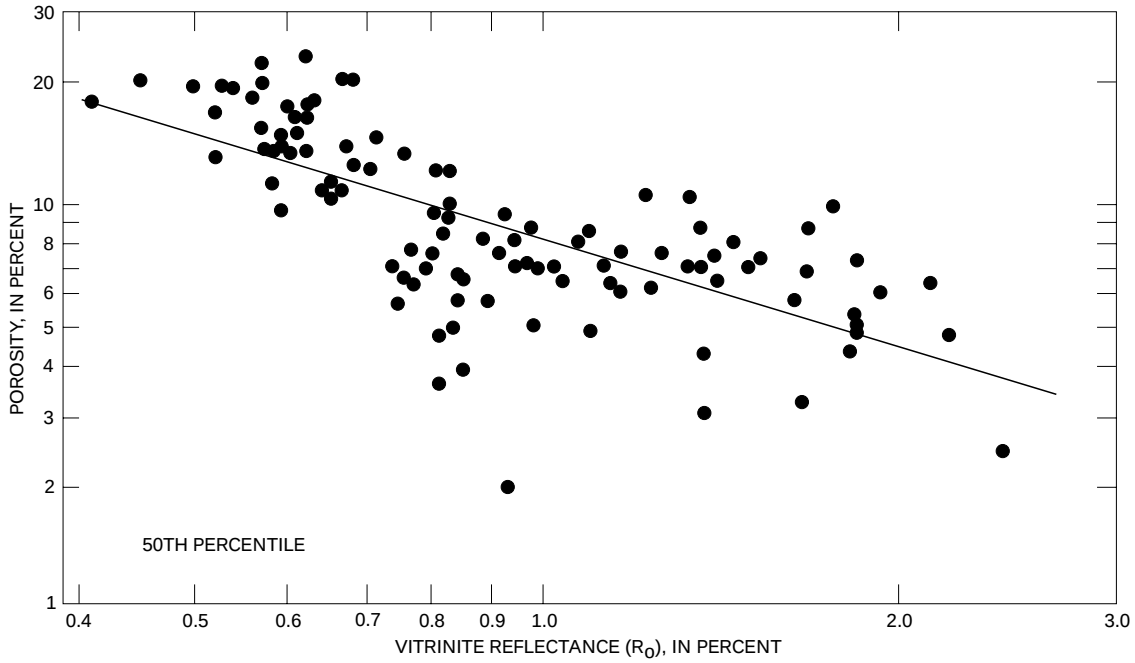

Figure 14. Porosity versus vitrinite reflectance for 50th percentile of Cretaceous sandstone data set, Rocky Mountain basins (table 2). Parameters for least-squares fit to data (line) are given in table 3.

in Rocky Mountain basins is shown in figure 18. This alternative predictive porosity framework is composed of two elements in order to represent the porosity–vitrinite reflectance data better than regression lines fit to the entire vitrinite reflectance range (fig. 17). The trend lines of models A (fig. 18*A*) and B (fig. 18*B*) are subjectively drawn, incorporating my ideas and biases, to fit the data of figures 12–16. Models A and B are derived from observation of porosity–vitrinite reflectance crossplot patterns and represent a working hypothesis that, because of a paucity of data, is at present supported only by circumstantial evidence.

Model A applies to strata in which porosity continues to decrease at a uniform rate as vitrinite reflectance increases

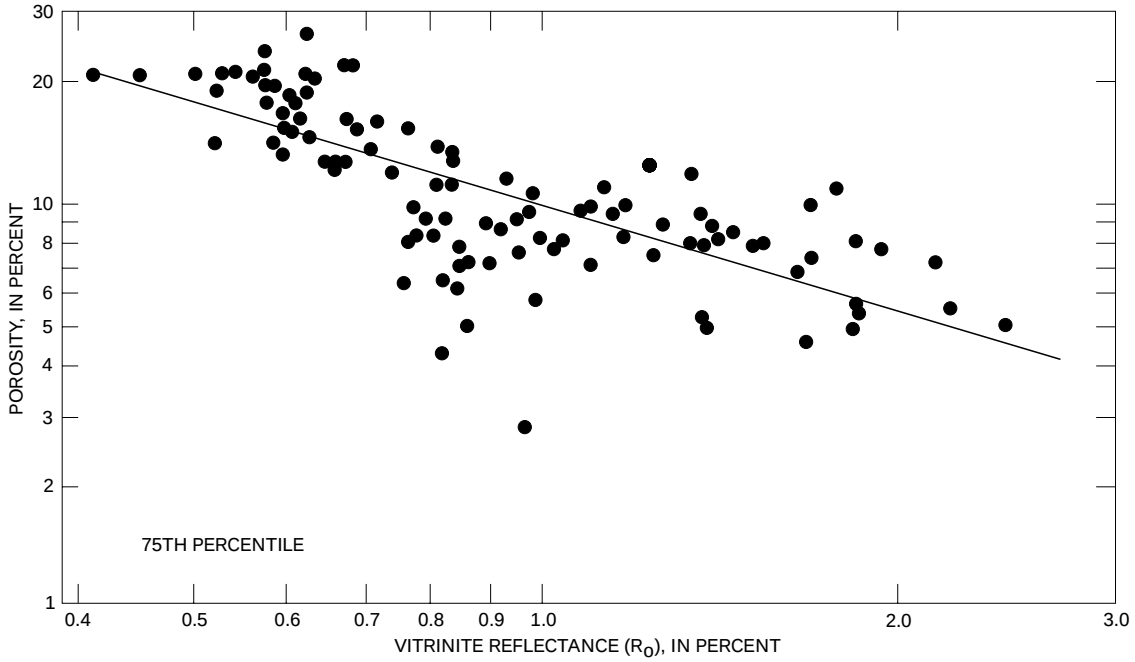

Figure 15. Porosity versus vitrinite reflectance for 75th percentile of Cretaceous sandstone data set, Rocky Mountain basins (table 2). Parameters for least-squares fit to data (line) are given in table 3.

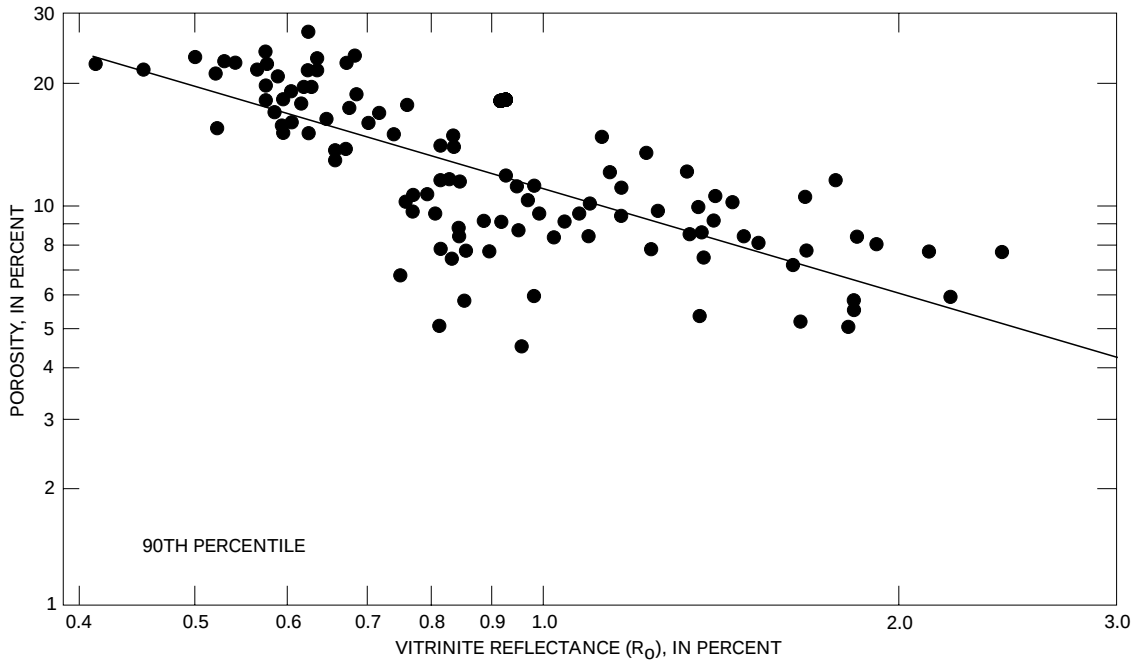

Figure 16. Porosity versus vitrinite reflectance for 90th percentile of Cretaceous sandstone data set, Rocky Mountain basins (table 2). Parameters for least-squares fit to data (line) are given in table 3.

above 0.9 percent. Model B applies to strata in which the rate of porosity loss slows as vitrinite reflectance increases above 0.9 percent. (The abrupt change in slope shown in figure 18*B* schematically represents a transition zone.) For vitrinite reflectance less than 0.9 percent, models A and B are identical.

Differences in models A and B do not directly reflect variability in rock properties such as grain size and sorting, shale content, composition of framework grains, and so on. The effects on porosity of these factors are already incorporated in the porosity range defined by the 10th through 90th porosity percentiles. Rather, models A and B are interpreted

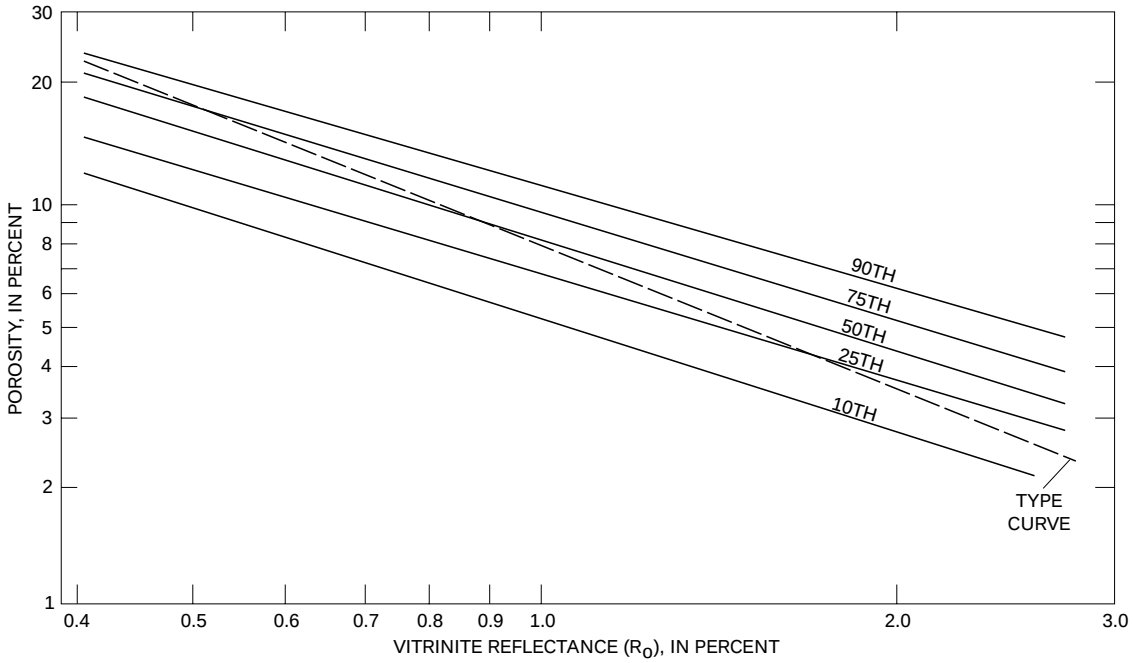

Figure 17. Summary figure showing regression lines representing 10th, 25th, 50th, 75th, and 90th porosity percentiles versus vitrinite reflectance shown in figures 12–16 for the Cretaceous sandstone data set, Rocky Mountain basins. These trend lines constitute a possible empirical, predictive porosity model for Cretaceous sandstones of the Rocky Mountain region. An alternative model is presented in figure 18. Dashed type curve (also shown in figures 7 and 18) provides a reference line that represents sandstones in general (Schmoker and Gautier, 1989).

as representing sandstones in which porosity evolution follows fundamentally different pathways.

The predictive porosity models of figure 17 and figure 18*A* are conceptually similar in that each line segment spans the entire thermal maturity range. Such models implicitly assume that the net effect on porosity of various diagenetic processes, operative at different levels of thermal maturity, can be approximated by single power functions over a large vitrinite reflectance range. This assumption does not seem obvious a priori but is empirically supported by a number of published data sets (Schmoker and Gautier, 1988, 1989; Schmoker and Hester, 1990; Schmoker and Higley, 1991). A single porosity–vitrinite reflectance power function spanning a large vitrinite reflectance range is analogous to a single porosity-depth exponential function spanning a large depth range (Schmoker and Gautier, 1988). Such porosity-depth exponential curves are common in the literature, although the underlying assumptions are rarely discussed.

The line segments of figure 18*B* change slope as vitrinite reflectance increases. Such porosity models implicitly assume that the net effect on porosity of various diagenetic processes varies as different processes wax and wane during burial. Figure 18*B* could not be depicted by a single exponential curve in the porosity-depth domain.

The choice of diagenetic pathway (model A versus model B) is important for sandstone porosity prediction in deep parts of Rocky Mountain basins. At 2.0 percent R_o, for example, model A predicts median porosities of about 2 percent and 90th-percentile porosities of only 4 percent; in contrast, model B predicts median porosities of about 5 percent and 90th-percentile porosities of 8 percent. Extrapolating beyond the data to 3.0 percent R_o, model A predicts 10th- through 90th-percentile porosities to all be less than 3 percent, whereas model B predicts some porosities of 6–7 percent. Reference to figure 11 shows that maximum depths of economic production predicted by model A in a given area of a basin would be thousands of feet less than those predicted by model B.

As is apparent from the foregoing porosity comparisons, the hypothesis that porosity evolution can follow distinctly different pathways as vitrinite reflectance increases above 0.9 percent has significant implications for the economic production of deeply buried hydrocarbons. Understanding which sandstones follow models analogous to A and which follow models analogous to B is important. At this point, however, such understanding is uncertain, and the following discussion of cause and effect is speculative.

The particular strata of the data set that conform to model B are from the Almond Formation in the Green River Basin and the Mesaverde Group (marine and nonmarine) in the Piceance Basin (table 2). Low-permeability sandstones in both formations are commonly overpressured at vitrinite

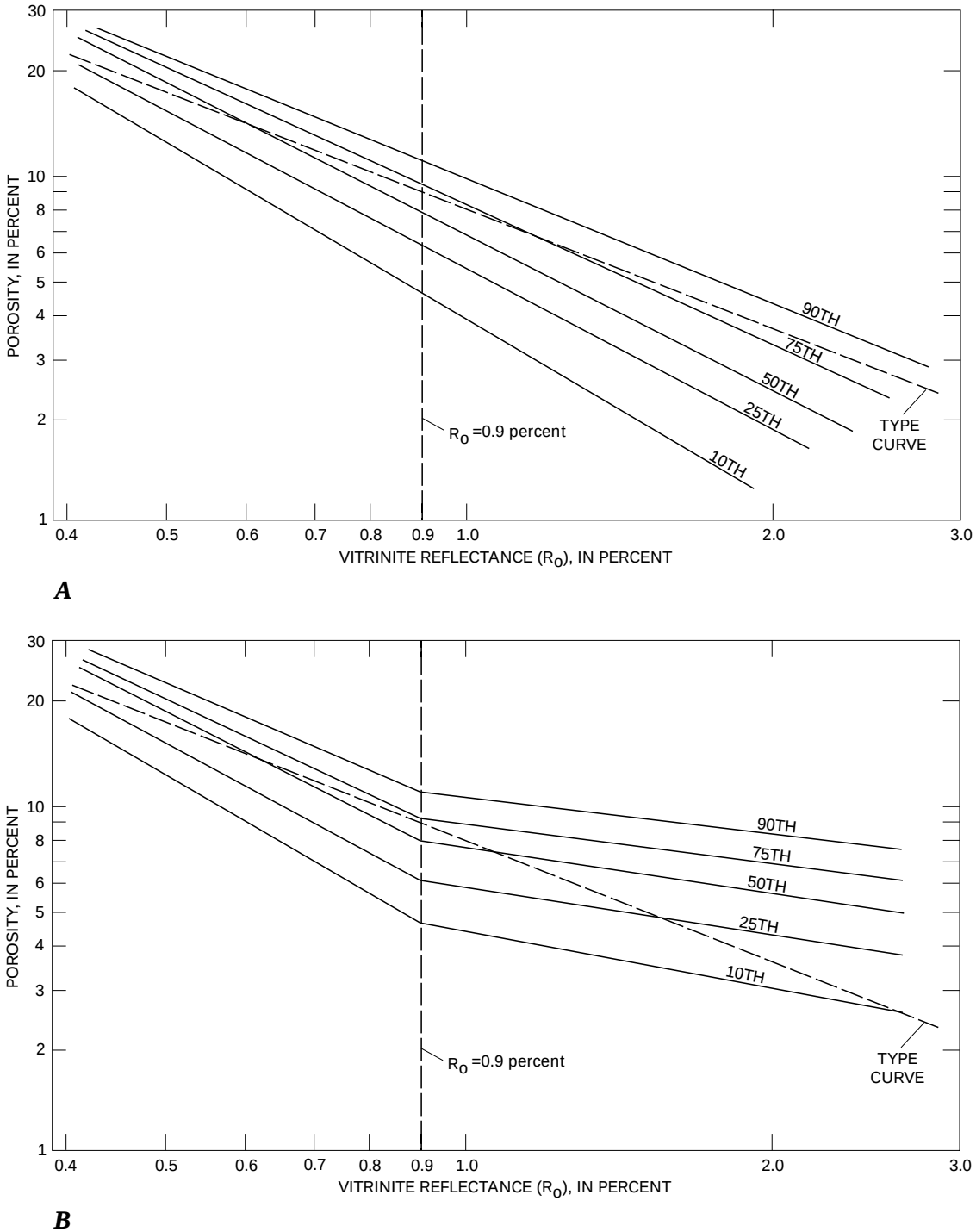

Figure 18. Subjectively drawn trend lines representing 10th, 25th, 50th, 75th, and 90th porosity percentiles versus vitrinite reflectance, Cretaceous sandstone data set, Rocky Mountain basins. These trend lines constitute an alternative predictive porosity model to the set of regression lines of figure 17. Dashed type curve (also shown in figures 7 and 17) provides a reference line that represents sandstones in general (Schmoker and Gautier, 1989). For vitrinite reflectance less than 0.9 percent, trend lines of *A* and *B* are identical and represent all data (figs. 12–16). For vitrinite reflectance greater than 0.9 percent, trend lines of *A* represent strata in which porosity continues to decrease at a uniform rate and trend lines of *B* represent strata in which the rate of porosity loss decreases.

reflectance greater than 0.9 percent due to hydrocarbon generation (Spencer, 1987). It is thus possible that some Cretaceous sandstones of Rocky Mountain basins do not follow normal diagenetic pathways (fig. 18*A*) because of the effects on diagenesis of hydrocarbon generation from adjacent and intercalated coals and organic-rich shales.

Hydrocarbon generation, of which overpressuring in the nonsubsiding basins of the Rocky Mountain region is evidential (Spencer, 1987), has the potential to retard porosity loss as vitrinite reflectance increases (fig. 18*B*) in at least three ways. First, hydrocarbons can inhibit cementation by displacing pore water. Second, carbon dioxide (Schmidt and McDonald, 1979) and organic acids (Surdam and others, 1989) produced by the thermal breakdown of kerogen can create secondary porosity by dissolving cements and framework grains. Third, overpressuring can slow pressure solution and associated porosity decrease by reducing the lithostatic load; overpressuring can also reduce cementation through development of a fluid-flow system characterized by expulsion, rather than exchange, of liquids.

If hydrocarbon generation is indeed the primary underlying process causing some sandstones to deviate from porosity–vitrinite reflectance trends similar to those of figure 18*A* and follow instead trends similar to those of figure 18*B*, then the results and discussion of this section are not restricted to Rocky Mountain Cretaceous sandstones.

SUMMARY AND CONCLUSIONS

Porosity descriptions are of limited value if progress is not made toward predictive models. In this report, I describe empirical porosity trends for which sandstone porosity is linked with thermal maturity, rock properties, and hydrocarbon generation. These parameters are useful in predictive porosity models because they commonly can often be anticipated in advance of the drill.

The overall decrease of sandstone porosity during burial is treated as a function of thermal maturity as represented by vitrinite reflectance. In this context, vitrinite reflectance serves as a generalized index of thermal history rather than as a specialized indicator of kerogen decomposition. Complicating the picture, however, the data show that the response of sandstone porosity to increasing thermal maturity may depend in part on the presence or absence of hydrocarbon generation and overpressuring.

The range of porosity at a given level of thermal maturity is not obscured here by averaging but is depicted by porosity–vitrinite reflectance trends representing the 10th, 25th, 50th, 75th, and 90th porosity percentiles. Effects on porosity of variations in rock properties are thus taken into account.

Data from Cretaceous sandstones of Rocky Mountain basins are used to illustrate and test methods for predicting the porosity and porosity range of sandstones. Most of these Cretaceous sandstones are not deeply buried, but the availability of porosity, vitrinite reflectance, and rock property data makes them useful formations for developing approaches to porosity prediction. These approaches can be applied to deeply buried sandstones in general.

REFERENCES CITED

Athy, L.F., 1930, Density, porosity, and compaction of sedimentary rocks: American Association of Petroleum Geologists Bulletin, v. 14, no. 1, p. 1–24.

Baldwin, Brewster, and Butler, C.O., 1985, Compaction curves: American Association of Petroleum Geologists Bulletin, v. 69, no. 4, p. 622–626.

Bloch, S., 1991, Empirical prediction of porosity and permeability in sandstones: American Association of Petroleum Geologists Bulletin, v. 75, no. 7, p. 1145–1160.

Cassan, J.P., Garcia-Palacios, M.C., Fritz, Bertrand, and Tardy, Yves, 1981, Diagenesis of sandstone reservoirs as shown by petrographical and geochemical analysis of oil bearing formations in the Gabon basin: Bulletin des Centres de Recherches Exploration-Production Elf-Aquitaine, Pau, France, v. 5, no. 1, p. 113–135.

Cleveland, W.S., 1985, The elements of graphing data: Monterey, California, Wadsworth Advanced Books and Software, 323 p.

Coalson, E.B., ed., 1989, Petrogenesis and petrophysics of selected sandstone reservoirs of the Rocky Mountain region: Denver, Rocky Mountain Association of Geologists, 353 p.

Hansley, P.L., and Johnson, R.C., 1980, Mineralogy and diagenesis of low-permeability sandstones of Late Cretaceous age, Piceance Creek basin, northwestern Colorado: The Mountain Geologist, v. 17, no. 4, p. 88–106.

Higley, D.K., and Schmoker, J.W., 1989, Influence of depositional environment and diagenesis on regional porosity trends in the Lower Cretaceous "J" sandstone, Denver basin, Colorado, *in* Coalson, E.B., ed., Petrogenesis and petrophysics of selected sandstone reservoirs of the Rocky Mountain region: Denver, Rocky Mountain Association of Geologists, p. 183–196, 334–335.

Houseknecht, D.W., 1984, Influence of grain size and temperature on intergranular pressure solution, quartz cementation, and porosity in a quartzose sandstone: Journal of Sedimentary Petrology, v. 54, no. 2, p. 348–361.

Keighin, C.W., and Fouch, T.D., 1981, Depositional environments and diagenesis of some nonmarine Upper Cretaceous reservoir rocks, Uinta basin, Utah, *in* Ethridge, F.G., and Flores, R.M., eds., Recent and ancient nonmarine depositional environments—Models for exploration: Society of Economic Paleontologists and Mineralogists Special Publication 31, p. 109–125.

Keighin, C.W., Law, B.E., and Pollastro, R.M., 1989, Petrology and reservoir characteristics of the Almond Formation, greater Green River basin, Wyoming, *in* Coalson, E.B., ed., Petrogenesis and petrophysics of selected sandstone reservoirs of the Rocky Mountain region: Denver, Rocky Mountain Association of Geologists, p. 281–298, 344–347.

Land, C.B., and Weimer, R.J., 1978, Peoria field, Denver basin, Colorado—J sandstone distributary channel reservoir, *in* Pruit, J.D., and Coffin, P.E., eds., Energy resources of the Denver basin: Denver, Rocky Mountain Association of Geologists, p. 81–104.

Lyons, D.J., 1978, Sandstone reservoirs: Petrography, porosity-permeability relationship, and burial diagenesis: Tokyo, Technology Research Center, Japan National Oil Corporation, Report 8, p. 1–69.

———1979, Organic metamorphism and sandstone porosity prediction from acoustic data: Tokyo, Technology Research Center, Japan National Oil Corporation, Report 9, p. 1–51.

Maxwell, J.C., 1964, Influence of depth, temperature, and geologic age on porosity of quartzose sandstone: American Association of Petroleum Geologists Bulletin, v. 48, no. 5, p. 697–709.

Pitman, J.K., Anders, D.E., Fouch, T.D., and Nichols, D.J., 1986, Hydrocarbon potential of nonmarine Upper Cretaceous and Lower Tertiary rocks, eastern Uinta basin, Utah, *in* Spencer, C.W., and Mast, R.F., eds., Geology of tight gas reservoirs: American Association of Petroleum Geologists Studies in Geology 24, p. 235–252.

Pitman, J.K., Franczyk, K.J., and Anders, D.E., 1987, Marine and nonmarine gas-bearing rocks in Upper Cretaceous Blackhawk and Neslen Formations, eastern Uinta basin, Utah—Sedimentology, diagenesis, and source rock potential: American Association of Petroleum Geologists Bulletin, v. 71, no. 1, p. 76–94.

———1988, Diagenesis and burial history of nonmarine Upper Cretaceous rocks in the central Uinta basin, Utah: U.S. Geological Survey Bulletin 1787–D, 24 p.

Scherer, M., 1987, Parameters influencing porosity in sandstones—A model for sandstone porosity prediction: American Association of Petroleum Geologists Bulletin, v. 71, no. 5, p. 485–491.

Schmidt, Volkmar, and McDonald, D.A., 1979, The role of secondary porosity in the course of sandstone diagenesis, *in* Scholle, P.A., and Schluger, P.R., eds., Aspects of diagenesis: Society of Economic Paleontologists and Mineralogists Special Publication 26, p. 175–207.

Schmoker, J.W., and Gautier, D.L., 1988, Sandstone porosity as a function of thermal maturity: Geology, v. 16, no. 11, p. 1007–1010.

———1989, Compaction of basin sediments: Modeling based on time-temperature history: Journal of Geophysical Research, v. 94(B), no. 6, p. 7379–7386.

Schmoker, J.S., and Hester, T.C., 1990, Regional trends of sandstone porosity versus vitrinite reflectance—A preliminary framework, *in* Nuccio, V.F., and Barker, C.E., eds., Applications of thermal maturity studies to energy exploration: Rocky Mountain Section, Society of Economic Paleontologists and Mineralogists, Denver, p. 53–60.

Schmoker, J.W., and Higley, D.K., 1991, Porosity trends of the Lower Cretaceous J sandstone, Denver basin, Colorado: Journal of Sedimentary Petrology, v. 61, no. 6, p. 909–920.

Schmoker, J.W., Nuccio, V.F., and Pitman, J.K., 1992, Porosity trends in predominantly nonmarine sandstones of the Upper Cretaceous Mesaverde Group, Uinta and Piceance basins, Utah and Colorado, *in* Fouch, T.D., Nuccio, V.F., and Chidsey, T.C., eds., Hydrocarbon and mineral resources of the Uinta basin, Utah and Colorado: Salt Lake City, Utah Geological Association Guidebook 20, p. 111–121.

Siever, Raymond, 1983, Burial history and diagenetic reaction kinetics: American Association of Petroleum Geologists Bulletin, v. 67, no. 4, p. 684–691.

Spencer, C.W., 1987, Hydrocarbon generation as a mechanism for overpressuring in Rocky Mountain region: American Association of Petroleum Geologists Bulletin, v. 71, no. 4, p. 368–388.

Spencer, C.W., and Keighin, C.W., eds., 1984, Geologic studies in support of the U.S. Department of Energy Multiwell Experiment, Garfield County, Colorado: U.S. Geological Survey Open-File Report 84–757, 134 p.

Surdam, R.C., Crossey, L.J., Hagen, E.S., and Heasler, H.P., 1989, Organic-inorganic interactions and sandstone diagenesis: American Association of Petroleum Geologists Bulletin, v. 73, no. 1, p. 1–23.

Tainter, P.A., 1984, Stratigraphic and paleostructural controls on hydrocarbon migration in Cretaceous D and J sandstones of the Denver basin, *in* Woodward, Jane, Meissner, F.F., and Clayton, J.L., eds., Hydrocarbon source rocks of the greater Rocky Mountain region: Denver, Rocky Mountain Association of Geologists, p. 339–354.

Till, Roger, 1974, Statistical methods for the earth scientist: New York, John Wiley, 154 p.

Tissot, B.P., and Welte, D.H., 1984, Petroleum formation and occurrence (2nd ed.): New York, Springer-Verlag, 699 p.

van de Kamp, P.C., 1976, Inorganic and organic metamorphism in siliciclastic rocks [abs.]: American Association of Petroleum Geologists Bulletin, v. 60, no. 4, p. 729.